Sensors and Actuators B 150 (2010) 200–205

Contents lists available at ScienceDirect

Sensors and Actuators B: Chemical

journal homepage: www.elsevier.com/locate/snb

Ag nanoparticles self-supported on $Ag_2V_4O_{11}$ nanobelts: Novel nanocomposite for direct electron transfer of hemoglobin and detection of H_2O_2

Chunliang Lu[a,b], Qingming Shen[a,c], Xiaomei Zhao[c], Junjie Zhu[c], Xuefeng Guo[a,*,1], Wenhua Hou[a,*]

[a] Key Laboratory of Mesoscopic Chemistry of MOE, School of Chemistry and Chemical Engineering, Nanjing University, Nanjing 210093, PR China
[b] Testing Center of Yangzhou University, Yangzhou University, Yangzhou 225009, PR China
[c] Key Laboratory of Analytical Chemistry for Life Science of MOE, School of Chemistry and Chemical Engineering, Nanjing University, Nanjing 210093, PR China

ARTICLE INFO

Article history:
Received 27 February 2010
Received in revised form 6 July 2010
Accepted 8 July 2010
Available online 16 July 2010

Keywords:
Nanocomposite
Ag
$Ag_2V_4O_{11}$
Hemoglobin
Biosensor
H_2O_2 detection

ABSTRACT

Nanocomposite of Ag nanoparticles self-supproted on $Ag_2V_4O_{11}$ nanobelts, prepared by γ-ray irradiation treatments of $Ag_2V_4O_{11}$ nanobelts, was used to immobilize hemoglobin on glassy carbon electrode. Detailed electrochemical analysis was performed and it was found that $Ag/Ag_2V_4O_{11}$ nanocomposite significantly improved the direct electron transfer between hemoglobin and glassy carbon electrode, leading to the fabrication of a biosensor with a very sensitive detection of H_2O_2. The apparent surface concentration (Γ^*) of hemoglobin and the electron transfer rate constant (k_s) were calculated to be 1.6×10^{-10} mol/cm^2 and 2.6 s^{-1}, respectively. The linear detection range of H_2O_2 was 1.0–120 μM, with a detection limit of 0.3 μM.

1. Introduction

Direct electrochemistry of redox proteins immobilized on nanomaterial-modified electrode has attracted much attention from electrochemical scientists in last few decades [1–5] since Eddowes and Hill [6] and Yeh and Kuwana [7] independently reported that the reversible electrochemistry was successfully realized via cytochrome *c* on gold electrode and on tin-doped indium oxide electrode respectively in 1977. The research on the direct electron transfer from protein to electrode surface can not only serve as a model to understand electron transfer mechanisms in biological systems that may elucidate the relationship between the structures and biological functions [8], but also establish a foundation for constructing the third-generation electrochemical biosensors [9], in which the redox mediators are no longer needed and the complications brought about by the mediators are avoided.

However, it is difficult for proteins to realize direct electron transfer on "bare" electrodes because of their easy denaturation, deeply embedded active centers, and frequently unfavorable orientations [10,11]. To maintain the native structures and appropriate orientations of redox proteins and thus to acquire an increased electron transfer between the protein and electrode, various supporting matrices such as surfactant, sol–gel, polymers and nanomaterials have been studied [12,13]. Among these different kinds of matrices, nanosized materials offer many advantages due to their unique size and special physical, chemical and electrochemical properties [14,15].

Heme proteins are important redox proteins that contain the porphyrin complex of iron(II) or hemin(III) as a prosthetic group. Among various heme proteins, hemoglobin (Hb) is an ideal model molecule for the study of electron transfer reactions of heme enzymes and also for biosensing and electrocatalysis [16] because of its known and documented structure, commercial availability and relatively inexpensiveness. Hemoglobin is a soft globular heme protein with a dimension of 5.3 nm × 5.4 nm × 6.5 nm and a molecular weight of approximately 64,500 g mol^{-1}. It consists of four subunits of polypeptide enzymes, every heme (iron porphyrin) group in each subunit acts as an active center [17].

Silver vanadium oxide (SVO) is a kind of potential cathode material for primary and secondary lithium ion batteries, and many efforts have been made in the preparation, characterization, and discharging and recharging behaviors of SVO [18–23]. Among numerous SVO phases that contain Ag, V, and O in a number of stoichiometric and nonstoichiometric ratios, $Ag_2V_4O_{11}$ has

* Corresponding author. Tel.: +86 25 83686001; fax: +86 25 83317761.
E-mail addresses: guoxf@nju.edu.cn (X. Guo), whou@nju.edu.cn (W. Hou).
[1] Tel.: +86 25 83686393; fax: +86 25 83317761.

0925-4005/$ – see front matter © 2010 Elsevier B.V. All rights reserved.
doi:10.1016/j.snb.2010.07.016

been investigated most extensively and was used as a commercial cathode material in primary lithium batteries for implantable biomedical devices [24]. $Ag_2V_4O_{11}$ can be easily synthesized by using different methods and starting materials. Recently, the hydrothermal method has also been introduced to the synthesis of SVO [25]. Compared with the traditional solid phase synthetic route, the hydrothermal process possesses many advantages such as low reaction temperature, short reaction time, easy post-treatment, energy saving, and environmental friendliness.

Silver nanoparticles are one kind of the most extensively investigated nanomaterials for their excellent performances such as chemical stability, catalytic activity, antibacterial ability, and nonlinear optic property [26–35]. In fact, besides silver nanoparticles, nanocomposites with silver nanoparticles as one component has also been drawing more and more attention owing to its potential applications in many fields. In 2008, Li et al. developed a one-pot synthetic method to prepare Ag/SVO nanocomposite with Ag nanoparticles supported on $AgVO_3$ nanobelts [36]. Very recently, our group also applied a facile post-treatment method for the preparation of $Ag/Ag_2V_4O_{11}$ nanocomposite with Ag nanoparticles self-supported on $Ag_2V_4O_{11}$ nanobelts [37].

The rapid, convenient and accurate determination of hydrogen peroxide (H_2O_2) is required in many fields such as industry, clinical control, and environmental protection [38,39]. Compared with the traditional techniques such as titrimetry and spectrophotometry [40,41], the electrochemical method is fast and easy, and has obvious advantages for the determination of H_2O_2 [4]. Heme proteins have peroxidase activity and can be used to reduce H_2O_2 through electrochemical catalysis.

In this work, by modifying glassy carbon electrode with $Ag/Ag_2V_4O_{11}$ nanocomposite, the direct electrochemistry of Hb was successfully realized, and a biosensor for the detection of H_2O_2 was constructed.

2. Experimental

2.1. Materials preparation

Bovine heart hemoglobin (Hb) was purchased from Sigma and used without further purification. Hydrogen peroxide (H_2O_2, 30 wt% aqueous solution) was obtained from Shanghai Biochemical Reagent Company. All other reagents were of analytical grade and used as received.

$Ag_2V_4O_{11}$ nanobelt was synthesized according to the literature [37] through a hydrothermal method. In a typical process, 1 mmol $AgNO_3$ was first dissolved into 20 mL distilled water under magnetic stirring, then 1 mmol V_2O_5 was added and ultrasonic radiation was employed for 30 min to get a suspension. The obtained suspension was then transferred into a Teflon-lined stainless steel autoclave, heated to 170 °C and aged for 12 h. After being naturally cooled to room temperature, the final product was collected by centrifugation, washed with distilled water repeatedly until the pH value of the centrifugate was about 6. Then the obtained precipitate was washed with absolute ethanol, centrifuged and finally dried in air at room temperature and $Ag_2V_4O_{11}$ nanobelt was thus obtained.

To obtain $Ag/Ag_2V_4O_{11}$ nanocomposite, the obtained $Ag_2V_4O_{11}$ nanobelt was irradiated by a certain dose of ^{60}Co γ-ray (Isotope Institute of Henan Academy of Sciences, the activity of the ^{60}Co γ-ray source is 7.4×10^{15} Bq), typically 20 kGy (1.0 g sample was sealed with PE film, located at the place where the dose rate is 200 Gy/min, and irradiated for 100 min). Under irradiation treatments, Ag nanoparticles were segregated at the surface of $Ag_2V_4O_{11}$ nanobelts and hence $Ag/Ag_2V_4O_{11}$ nanocomposite was formed [37].

For the construction of biosensor, 2 mg $Ag/Ag_2V_4O_{11}$ nanocomposite was first dispersed in 2 mL double distilled water (abbreviated as ddH_2O), then 2 mL of the stock solution of Hb (2 mg/mL, 0.1 M phosphate-buffered solution [PBS], pH 7.0) was added and the mixture was equilibrated for 24 h at room temperature and centrifuged to collect the solid. The resulting $Hb/Ag/Ag_2V_4O_{11}$ composite was used for further testing.

Glassy carbon electrode (GCE) was first polished with 1.0 μm, 0.3 μm, and 0.05 μm alumina powder successively, followed by rinsing thoroughly with ddH_2O. The polished electrode was then sonicated in ddH_2O and acetone, and finally allowed to dry at room temperature.

The $Hb/Ag/Ag_2V_4O_{11}$ composite mentioned above was resuspended in 1 mL water, and 5 μL of this suspension was deposited onto the electrode surface. The electrode was then left to dry at 4 °C for at least 24 h. The sensor was stored under the same conditions when not in use.

2.2. Characterization and electrochemistry measurements

Powder X-ray diffraction patterns were obtained on a Philips X'Pert MPD Pro X-ray diffractometer operated with graphite-monochromatized high intensity Cu Kα radiation at 50 kV. Transmittance electron microspectroscopy (TEM) images were recorded with a JEOL JEM-100S electron microscope at an accelerating voltage of 80 kV. Cyclic voltammetric experiments were conducted with a CHI660B workstation (Shanghai Chenhua). All experiments were carried out using a conventional three-electrode system, where GCE modified with $Hb/Ag/Ag_2V_4O_{11}$ was used as working electrode, a platinum wire was used as auxiliary electrode, and a saturated calomel electrode (SCE) was used as reference electrode. All solutions were deoxygenated by highly pure nitrogen before and during the measurements.

3. Results and discussion

3.1. XRD and TEM analysis

The powder XRD pattern of the as-prepared $Ag_2V_4O_{11}$ belt matches well with that reported previously [37]. A typical TEM image of $Ag/Ag_2V_4O_{11}$ nanocomposite obtained by γ-ray treatment of $Ag_2V_4O_{11}$ nanobelt is shown in Fig. 1. It can be seen that the silver nanoparticles are well dispersed on the surface of $Ag_2V_4O_{11}$ nanobelts and their diameters vary from 10 nm to 50 nm.

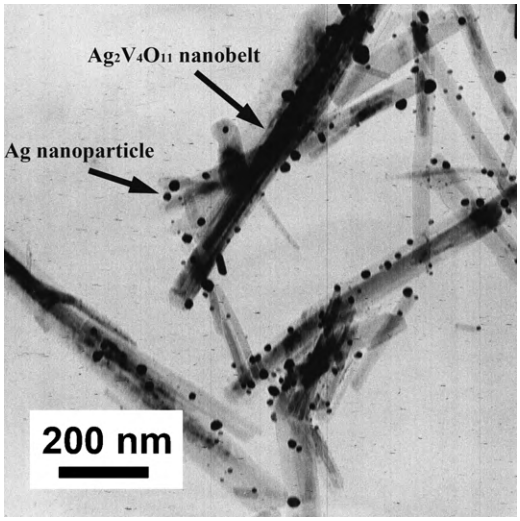

Fig. 1. TEM image of $Ag/Ag_2V_4O_{11}$ nanocomposite.

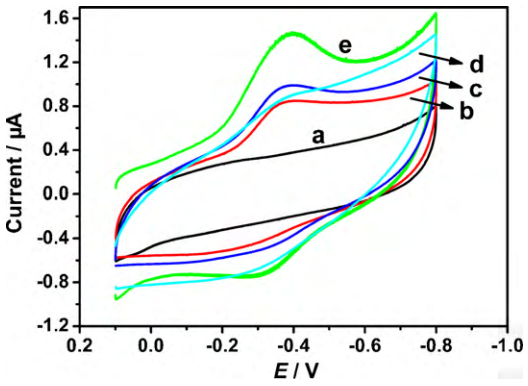

Fig. 2. Cyclic voltammograms of (a) $Ag/Ag_2V_4O_{11}$/GCE, (b) Hb/GCE, (c) Hb/Ag/GCE, (d) $Hb/Ag_2V_4O_{11}$/GCE, and (e) $Hb/Ag/Ag_2V_4O_{11}$/GCE in 0.1 M PBS (pH 7.0) at a scan rate of 100 mV/s.

3.2. Direct electrochemistry of $Hb/Ag/Ag_2V_4O_{11}$ modified electrode

The cyclic voltammograms (CVs) of different electrodes at a scan rate of 100 mV/s are given in Fig. 2. No peak appears at the electrode modified by $Ag/Ag_2V_4O_{11}$ nanocomposite, indicating that $Ag/Ag_2V_4O_{11}$ nanocomposite itself is not electroactive. When the electrode was modified with Hb, only a small irreversible reduction peak was observed and the reduction current was decreased with the number of cycles, suggesting the possible Hb denaturation and desorption over time on electrode surface as well as the non-reversible electrochemical reaction of Hb. However, at the $Hb/Ag/Ag_2V_4O_{11}$ modified electrode, a couple of well-defined redox peaks were observed at −0.372 V and −0.326 V, respectively, and the formal potential is calculated to be −0.349 V. The value of formal potential is quite close to that of Hb in agarose hydrogel film, −0.348 V [42], and ZnO-MWCNTs/Nafion film, −0.353 V [43].

For comparison, CVs of Hb/Ag modified GCE and $Hb/Ag_2V_4O_{11}$ modified GCE are also shown in Fig. 2. At the Hb/Ag modified GCE, the CV curve is almost the same as Hb modified GCE, but the reduction peak current is much bigger than the latter. Obviously, the co-existed Ag nanoparticles significantly improved the direct electron transfer between Hb and GCE. This can be explained by the high electronic conductivity and excellent biocompatibility of Ag nanoparticles [27,30]. However, at the $Hb/Ag_2V_4O_{11}$ modified GCE, although the reduction peak current is close to that of Hb modified GCE, its redox peaks are not as well-defined as the latter. In fact, it is very hard to identify its reduction peak. This phenomenon may be ascribed to the high electronic conductivity and poor biocompatibility of $Ag_2V_4O_{11}$ nanobelts [19].

Comparing all the CVs shown in Fig. 2, one can easily find that the $Hb/Ag/Ag_2V_4O_{11}$ modified GCE exhibits the best performance. This result presents strong evidence that the direct electron transfer between Hb and GCE can be greatly improved by the co-existence of $Ag/Ag_2V_4O_{11}$ nanocomposite.

A schematic diagram illustrating the microstructures of Hb modified GCE and $Hb/Ag/Ag_2V_4O_{11}$ modified GCE is shown in Fig. 3. On the surface of Hb modified GCE, in despite of the multilayer assembly of Hb molecules, only one or two layers of Hb which is very close to the electrode surface could realize direct electron transfer to and from the electrode and hence show their electrochemical activity (blue spheres emphasized with red circles), leaving most of the Hb molecules in the multilayers electrochemically nonactive (blue spheres).

However, in the case of $Hb/Ag/Ag_2V_4O_{11}$ modified GCE, the co-existed $Ag/Ag_2V_4O_{11}$ nanocomposites crossly contact with each other and thus a network which accommodates Hb molecules is formed. Because of the high electronic conductivity of $Ag_2V_4O_{11}$ [19] and Ag [27] as well as the biocompatibility of Ag [30], one can reasonably suppose that $Ag/Ag_2V_4O_{11}$ nanocomposite is both electronic conductive and biocompatible. Hence the network composed of $Ag/Ag_2V_4O_{11}$ nanocomposites could be a good matrix for the immobilization of biomolecules. Through the network matrix, Hb molecules that are directly contacted with $Ag/Ag_2V_4O_{11}$ nanocomposite are able to exchange electrons with GCE, showing electrochemical activity. Here $Ag/Ag_2V_4O_{11}$ nanocomposite plays the role of electronic bridge through which electrons are transferred from Hb to GCE or vice versa. Taking into account the much larger surface area of the network (compared with bare electrode), it is obvious that a great number of Hb molecules can transfer electrons to and from GCE indirectly and thus demonstrates their electrochemical activity.

In the above discussion, the orientations of Hb molecules are not taken into consideration. In fact, Hb molecules adopt random orientations on the surface of either GCE or $Ag/Ag_2V_4O_{11}$ nanocomposite. The possibilities of a favorable orientation of Hb on both surfaces are supposed to be equal because their space geometries are both global sphere referenced to a flat plane. Thus the specific value of the possibility is not the essential factor in the above discussion.

In summary, it is the conductive and biocompatible network of $Ag/Ag_2V_4O_{11}$ in which Hb molecules are accommodated that greatly improved the direct electron transfer between Hb and GCE. And the relatively lower electrochemical activity of Hb on Ag modified GCE and $Ag_2V_4O_{11}$ modified GCE can consequently be explained as follows. Ag nanoparticles are both conductive and biocompatible, but their small size and spherical shape make them difficult to form a network, hence the improvement effect of Ag nanoparticles is limited. On the other hand, $Ag_2V_4O_{11}$ nanobelts can construct a conductive network to accommodate Hb molecules, but their biocompatibility is poor. Thus Hb molecules may be denaturized and the improvement effect of $Ag_2V_4O_{11}$ nanobelts is even more limited.

To further examine the direct electron transfer behavior between Hb and $Ag/Ag_2V_4O_{11}$ modified GCE, different scan rates were applied and the corresponding CVs are shown in Fig. 4. The electrode modified with $Hb/Ag/Ag_2V_4O_{11}$ shows well-defined peaks at different scan rates from 20 mV/s to 1000 mV/s. With the increase of scan rate, the redox peak currents of the $Hb/Ag/Ag_2V_4O_{11}$ modified electrode increase linearly, indicating a surface-controlled electrochemical process.

For thin-layer electrochemistry, the integration of CV peak gives the total amount of charge (Q) passed through the electrode for reduction or oxidation of electroactive species in the thin film. The apparent surface concentration (Γ^*) of electroactive species can be

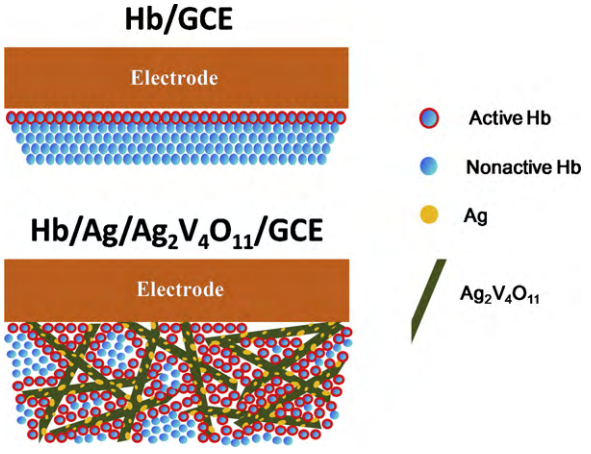

Fig. 3. A schematic diagram sketching the microstructrues of Hb modified GCE and $Hb/Ag/Ag_2V_4O_{11}$ modified GCE.

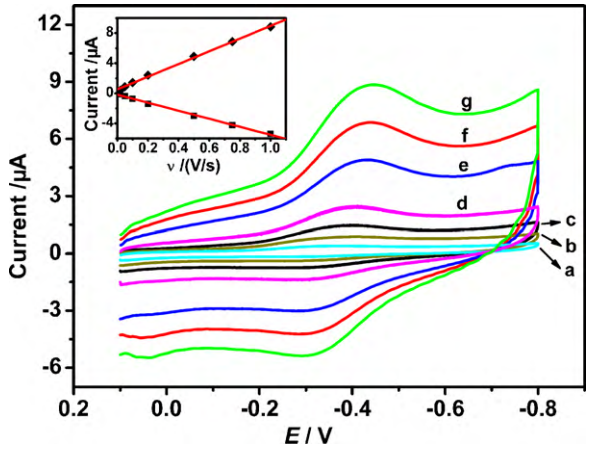

Fig. 4. Cyclic voltammograms of Hb/Ag/$Ag_2V_4O_{11}$ modified GCE in 0.1 M PBS (pH 7.0) at different scan rates: (a) 20 mV/s, (b) 50 mV/s, (c) 100 mV/s, (d) 200 mV/s, (e) 500 mV/s, (f) 750 mV/s, and (g) 1000 mV/s. Inset shows plot of peak current versus scan rate.

calculated from the following equation:

$$Q = nFA\Gamma^*$$

where n is the number of electrons transferred per biomolecule, F is Faraday's constant, and A is the electrode area. According to the equation, the average surface coverage of Hb was calculated to be 1.6×10^{-10} mol/cm^2 for the Hb/Ag/$Ag_2V_4O_{11}$ modified GCE. The value is more than 8 times of the theoretical monolayer coverage of Hb ($\sim 1.89 \times 10^{-11}$ mol/cm^2) on the basis of the crystallographic dimensional structure of Hb and assuming that the biomolecule adopts an orientation with the long axis parallel to the electrode surface [44]. The striking big surface coverage can be ascribed to the co-existence of Ag/$Ag_2V_4O_{11}$ nanocomposites which play the role of electronic bridges and connect more Hb molecules with the electrode, indicating that multilayers of Hb participate in the electron transfer process. The crossly contacted Ag/$Ag_2V_4O_{11}$ nanocomposites form a matrix with a high electronic conductivity and greatly expand the surface area of the electrode, leading to a much larger interacting surface between the electrode and Hb multilayers.

A small peak-to-peak separation always indicates a fast electron transfer rate. The electron transfer rate constant k_s can be estimated by the Laviron equation [45]:

$$\log k_s = \alpha \log(1-\alpha) + (1-\alpha)\log\alpha - \log\left(\frac{RT}{nF\nu}\right) - \frac{\alpha(1-\alpha)nF\Delta E_p}{2.3RT}$$

where α is the charge transfer coefficient, R is the gas constant, T is the absolute temperature, ΔE_p is the peak potential separation, and ν is the scan rate. A graph of the peak potential versus the logarithm of the scan rate yields a straight line (not shown), and from the slope of which a charge transfer coefficient of 0.45 was estimated for Hb. The peak-to-peak separations were 46 mV, 58 mV, 81 mV, and 87 mV at scan rates of 100 mV/s, 200 mV/s, 500 mV/s, and 750 mV/s respectively, giving an average k_s value of 2.6 s^{-1}. This value is much larger than the electron transfer rate constant of Hb in ZnO-MWCNTs/Nafion film (1.14 s^{-1}) [43], α-ZrP (1.85 s^{-1}) [46], silica-coated gold nanorods (0.83 s^{-1}) [47], and Au-SBA-15 (0.8 s^{-1}) [48], showing that the electron transfer between Hb in the matrix of Ag/$Ag_2V_4O_{11}$ nanocomposite and GCE is facile. This can be explained by the bridging effect of Ag/$Ag_2V_4O_{11}$ nanocomposite due to the excellent electronic conductivity, good biocompatibility and large surface area of Ag/$Ag_2V_4O_{11}$ nanocomposite network.

For comparison, CVs of Hb/Ag/GCE and Hb/$Ag_2V_4O_{11}$/GCE at different scan rates are shown in Figs. 5 and 6. From Fig. 5, the apparent surface concentration (Γ^*) of Hb and electron transfer constant (k_s)

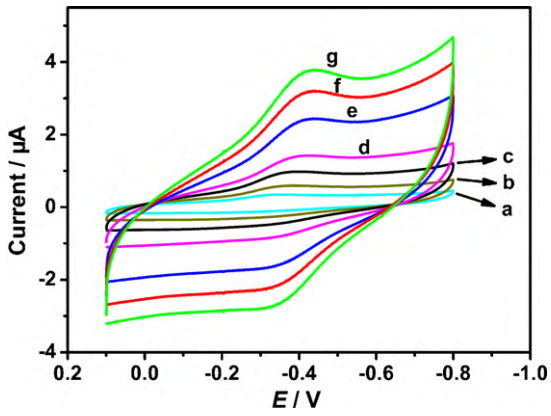

Fig. 5. Cyclic voltammograms of Hb/Ag modified GCE in 0.1 M PBS (pH 7.0) at different scan rates: (a) 20 mV/s, (b) 50 mV/s, (c) 100 mV/s, (d) 200 mV/s, (e) 500 mV/s, (f) 750 mV/s, and (g) 1000 mV/s.

are calculated to be 5.2×10^{-11} mol/cm^2 (about 2.8 times of monolayer coverage) and 1.4 s^{-1}, respectively. Both values are smaller than those for Hb/Ag/$Ag_2V_4O_{11}$/GCE, confirming that Ag/$Ag_2V_4O_{11}$ nanocomposite is a better matrix than Ag nanoparticles for Hb immobolization. In Fig. 6, redox peaks are not well-defined and both Γ^* and k_s are unable to be calculated, suggesting that Hb might be denaturized and that $Ag_2V_4O_{11}$ nanobelt is not a good matrix for Hb immobolization.

3.3. Influence of solution pH on the direct electron transfer of Hb

In order to further study the electron transfer behavior of Hb/Ag/$Ag_2V_4O_{11}$ modified GCE, the influence of solution pH on the direct electron transfer of Hb was also examined. An increase of solution pH caused a negative shift of both cathodic and anodic peak potentials, and all changes in voltammetric peak potentials and currents with pH were reversible. For example, the CV for the Hb/Ag/$Ag_2V_4O_{11}$/GCE at pH 9.0 was reproduced after immersion in pH 4.0 buffer and then returned to the pH 9.0 buffer. The increase of pH also resulted in a negative shift of the formal potential ($E^{0'}$) accordingly, in agreement with that reported previously. As shown in Fig. 7, the $E^{0'}$ of the heme Fe(III)/Fe(II) redox couple for the Hb/Ag/$Ag_2V_4O_{11}$ modified electrodes has a linear relationship with pH in the range of 4.0–8.0 and a slope of −45.8 mV pH^{-1}. This value is much smaller than −57.8 mV pH^{-1} at 18 °C for a reversible one-proton coupled single-electron transfer during electrochemical reduction. This may be due to the effect of the protonation states

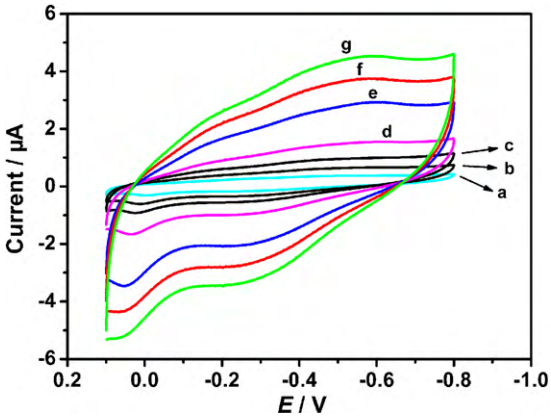

Fig. 6. Cyclic voltammograms of Hb/$Ag_2V_4O_{11}$ modified GCE in 0.1 M PBS (pH 7.0) at different scan rates: (a) 20 mV/s, (b) 50 mV/s, (c) 100 mV/s, (d) 200 mV/s, (e) 500 mV/s, (f) 750 mV/s, and (g) 1000 mV/s.

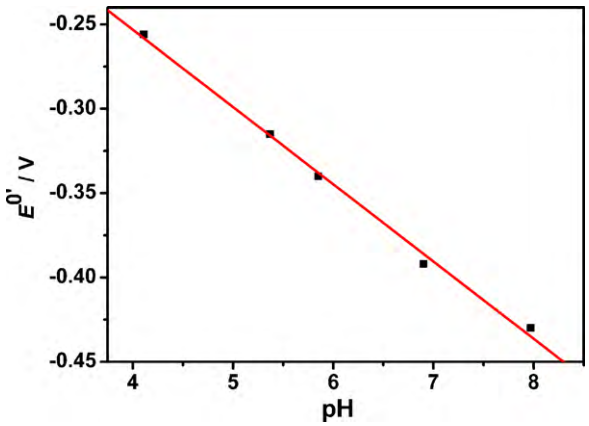

Fig. 7. Influence of solution pH on the formal potential of Hb/Ag/$Ag_2V_4O_{11}$ modified GCE.

of trans ligands to the heme iron and amino acids around the heme or to the protonation of water molecules coordinated to the center that may exist in different states under different pH values. Thus, the reaction equation for the electrochemical reduction of Hb may be described as follows:

$$\text{Hb heme Fe(III)} + H^+ + e^- \leftrightarrow \text{Hb heme Fe(II)}$$

3.4. Electrocatalysis of Hb/Ag/$Ag_2V_4O_{11}$/GCE to the reduction of H_2O_2

Heme proteins have peroxidase activity and can be used to reduce H_2O_2 through electrochemical catalysis. Based on the excellent electrochemical behaviors of Hb/Ag/$Ag_2V_4O_{11}$ modified GCE, it was applied to construct a biosensor for the detection of H_2O_2 in aqueous solution.

The CVs of Hb/Ag/$Ag_2V_4O_{11}$ modified electrode in 0.1 M PBS (pH 7.0) with different concentrations of H_2O_2 are shown in Fig. 8. The reduction peak current increased and the anodic peak current decreased dramatically with the addition of H_2O_2 on the Hb/Ag/$Ag_2V_4O_{11}$ modified electrode. Moreover, the currents of the reduction peaks increased with the increase of H_2O_2 concentration, indicating a typical electrocatalytic reduction process.

The reduction peak currents have a linear response to H_2O_2 concentration in the range of 1.0–120 μM with a detection limit of 0.3 μM (n = 13, R = 0.999, inset in Fig. 5). The relative standard deviation (RSD) of the peak current in six successive determinations at an H_2O_2 concentration of 1.0 μM was 4.98% for Hb/Ag/$Ag_2V_4O_{11}$ modified GCE.

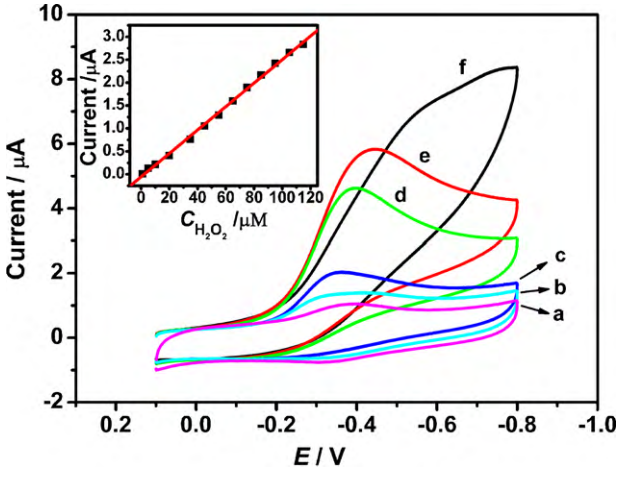

Fig. 8. Cyclic voltammograms of Hb/Ag/$Ag_2V_4O_{11}$/GCE with different H_2O_2 concentrations in 0.1 M PBS (pH 7.0) at a scan rate of 100 mV/s: (a) 0 μM, (b) 1 μM, (c) 10 μM, (d) 50 μM, (e) 100 μM, and (f) 200 μM. Inset shows plot of catalytic current versus H_2O_2 concentration.

Table 1
Linear range and detection limit of H_2O_2 for some Hb based electrodes.

Matrix	Linear range (μM)	Detection limit (μM)
Ag/$Ag_2V_4O_{11}$[a]	1.0–120	0.3
ZnO-MWCNTs/Nafion [43]	0.2–12	0.084
α-ZrP [46]	0.2–10.8	0.07
Carbon nanotube [49]	210–900	9

[a] This work.

4. Conclusions

The direct electron transfer between hemoglobin and glassy carbon electrode can be greatly improved by the modification of Ag/$Ag_2V_4O_{11}$ nanocomposite. With the aid of Ag/$Ag_2V_4O_{11}$ nanocomposite, the apparent surface concentration (Γ^*) of Hb on the electrode surface is calculated to be 1.6×10^{-10} mol/cm^2, more than 8 times of the theoretical monolayer coverage of Hb, and the electron transfer rate constant k_s is estimated to be 2.6 s^{-1}, also much larger than previously reported values. In addition, the biosensor of Hb/Ag/$Ag_2V_4O_{11}$ modified GCE exhibits a good electrocatalytic response for monitoring H_2O_2 and has a large linear detection range from 1.0 μM to 100 μM with a detection limit of 0.3 μM in the pH 7.0 solution. The fast electron transfer rate and excellent catalytic ability to the reduction of H_2O_2 also show that the protein retains its bioactivity well. The excellent performances may be ascribed to the unique electronic conductivity of $Ag_2V_4O_{11}$ nanobelts and biocompatibility of Ag nanoparticles. The matrix of Ag/$Ag_2V_4O_{11}$ nanocomposite may provide a new platform for the realization of direct electron transfer of biomolecules and the construction of biosensors.

Acknowledgements

This project was supported by the National Natural Science Foundation of China (Grant Nos.20773065, 20773062, 20403008), National Basic Research (973) Program of China (Grant No. 2009CB623504) and the Modern Analysis Center of Nanjing University.

References

[1] X.H. Chen, J.Q. Hu, Z.W. Chen, X.M. Feng, A.Q. Li, Nanoplated bismuth titanate sub-microspheres for protein immobilization and their corresponding direct electrochemistry and electrocatalysis, Biosens. Bioelectron. 24 (2009) 3448–3454.
[2] X. Chen, C.L. Fu, W.S. Yang, Graphite nanosheet-based composites for mediator-free H_2O_2 biosensor, Analyst 134 (2009) 2135–2140.
[3] D. Shan, G.X. Cheng, D.B. Zhu, H.G. Xue, S. Cosnier, S.N. Ding, Direct electrochemistry of hemoglobin in poly (acrylonitrile-co-acrylic acid) and its catalysis to H_2O_2, Sens. Actuators, B 137 (2009) 259–265.
[4] Q. Lu, T. Zhou, S.S. Hu, Direct electrochemistry of hemoglobin in PHEA and its catalysis to H_2O_2, Biosens. Bioelectron. 22 (2007) 899–904.
[5] J.W. Shie, U. Yogeswaran, S.M. Chen, Haemoglobin immobilized on nafion modified multi-walled carbon nanotubes for O_2, H_2O_2 and CCl_3COOH sensors, Talanta 78 (2009) 896–902.
[6] M.J. Eddowes, H.A.O. Hill, Novel method for the investigation of the electrochemistry of metalloproteins: Cytochrome *c*, J. Chem. Soc., Chem. Commun. 21 (1977) 771b–772b.
[7] P. Yeh, T. Kuwana, Reversible electrode-reaction of cytochrome-*c*, Chem. Lett. 10 (1977) 1145–1148.

[8] J. Wang, Electrochemical glucose biosensors, Chem. Rev. 108 (2008) 814–825.
[9] J.B. Jia, B.Q. Wang, A.G. Wu, G.J. Cheng, Z. Li, S.J. Dong, A method to construct a third-generation horseradish peroxidase biosensor: self-assembling gold nanoparticles to three-dimensional sol–gel network, Anal. Chem. 74 (2002) 2217–2223.
[10] A. Heller, Electrical wiring of redox enzymes, Acc. Chem. Res. 23 (1990) 128–134.
[11] Y. Liu, M.K. Wang, F. Zhao, Z.A. Xu, S.J. Dong, The direct electron transfer of glucose oxidase and glucose biosensor based on carbon nanotubes/chitosan matrix, Biosens. Bioelectron. 21 (2005) 984–988.
[12] F. Wang, X.X. Chen, Y.X. Xu, S.S. Hu, Z.N. Gao, Enhanced electron transfer for hemoglobin entrapped in a cationic gemini surfactant films on electrode and the fabrication of nitric oxide biosensor, Biosens. Bioelectron. 23 (2007) 176–182.
[13] J.W. Li, C. Fan, F. Xiao, R. Yan, S.S. Fan, F.Q. Zhao, B.Z. Zeng, Influence of ionic liquids on the direct electrochemistry of glucose oxidase entrapped in nanogold-N, N-dimethylformamide-ionic liquid composite film, Electrochim. Acta 52 (2007) 6178–6185.
[14] J.W. Di, S.H. Peng, C.P. Shen, Y.S. Gao, Y.F. Tu, One-step method embedding superoxide dismutase and gold nanoparticles in silica sol–gel network in the presence of cysteine for construction of third-generation biosensor, Biosens. Bioelectron. 23 (2007) 88–94.
[15] D. Du, X. Huang, J. Cai, A.D. Zhang, Amperometric detection of triazophos pesticide using acetylcholinesterase biosensor based on multiwall carbon nanotube-chitosan matrix, Sens. Actuators B 127 (2007) 531–535.
[16] C.X. Cai, J. Chen, Direct electron transfer and bioelectrocatalysis of hemoglobin at a carbon nanotube electrode, Anal. Biochem. 325 (2004) 285–292.
[17] S.G. Peng, Q.M. Gao, Q.G. Wang, J.L. Shi, Layered structural heme protein magadiite nanocomposites with high enzyme-like peroxidase activity, Chem. Mater. 16 (2004) 2675–2684.
[18] K.J. Takeuchi, A.C. Marschilok, S.M. Davis, R.A. Leising, E.S. Takeuchi, Silver vanadium oxides and related battery applications, Coord. Chem. Rev. 219 (2001) 283–310.
[19] S.Y. Zhang, W.Y. Li, C.S. Li, J. Chen, Synthesis, characterization, and electrochemical properties of $Ag_2V_4O_{11}$ and $AgVO_3$ 1-D nano/microstructures, J. Phys. Chem. B 110 (2006) 24855–24863.
[20] F. Huang, Z.W. Fu, Q.Z. Qin, A novel $Li_2Ag_{0.5}V_2O_5$ composite film cathode for all-solid-state lithium batteries, Electrochem. Commun. 5 (2003) 262–266.
[21] K.J. Takeuchi, R.A. Leising, M.J. Palazzo, A.C. Marschilok, E.S. Takeuchi, Advanced lithium batteries for implantable medical devices: mechanistic study of SVO cathode synthesis, J. Power Sources 119 (2003) 973–978.
[22] S.J. Bao, Q.L. Bao, C.M. Li, T.P. Chen, C.Q. Sun, Z.L. Dong, Y. Gan, J. Zhang, Synthesis and electrical transport of novel channel-structured β-$AgVO_3$, Small 3 (2007) 1174–1177.
[23] G.Z. Shen, D. Chen, Self-coiling of $Ag_2V_4O_{11}$ nanobelts into perfect nanorings and microloops, J. Am. Chem. Soc. 128 (2006) 11762–11763.
[24] A.M. Crespi, S.K. Somdahl, C.L. Schmidt, P.M. Skarstad, Evolution of power sources for implantable cardioverter defibrillators, J. Power Sources 96 (2001) 33–38.
[25] C.J. Mao, X.C. Wu, H.C. Pan, J.J. Zhu, H.Y. Chen, Single-crystalline $Ag_2V_4O_{11}$ nanobelts: hydrothermal synthesis, field emission, and magnetic properties, Nanotechnology 16 (2005) 2892–2896.
[26] S Mohapatra, Y.K. Mishra, J. Ghatak, D. Kabiraj, D.K. Avasthi, Surface plasmon resonance of Ag nanoparticles embedded in partially oxidized amorphous Si matrix, J. Nanosci. Nanotechnol. 8 (2008) 4285–4289.
[27] S.E. Kim, J.U. Kim, Y.H. Han, B.C. Lee, J.C. Lee, Size Controlled miniscale synthesis of silver nanoparticles using TEM electron beam, J. Nanosci. Nanotechnol. 8 (2008) 5212–5215.
[28] L. Faucher, E.F. Borra, A.M. Ritcey, Use of thiols as protecting ligands in reflective surface films of silver nanoparticles, J. Nanosci. Nanotechnol. 8 (2008) 3900–3908.
[29] Z.L. Wang, Oxide nanobelts and nanowires—growth, properties and applications, J. Nanosci. Nanotechnol. 8 (2008) 27–55.
[30] R.D. Deshmukh, R.J. Composto, Surface segregation and formation of silver nanoparticles created in situ in poly (methyl methacrylate) films, Chem. Mater. 19 (2007) 745–754.
[31] K. Esumi, T. Tano, K. Torigoe, K. Meguro, Preparation and characterization of bimetallic palladium–copper colloids by thermal decomposition of their acetate compounds in organic solvents, Chem. Mater. 2 (1990) 564–567.
[32] A. Taleb, V. Russier, A. Courty, M.P. Pileni, Optical anisotropy of organized silver nanoparticles in 2D superlattice, Appl. Surf. Sci. 162 (2000) 655–661.
[33] A. Henglein, Reduction of $Ag(CN)^{2-}$ on silver and platinum colloidal nanoparticles, Langmuir 17 (2001) 2329–2333.
[34] P.C. Lee, D. Meisel, Adsorption and surface-enhanced Raman of dyes on silver and gold sols, J. Phys. Chem. 86 (1982) 3391–3395.
[35] K.C. Grabar, R.G. Freeman, M.B. Hommer, M.J. Natan, Preparation and characterization of Au colloid monolayers, Anal. Chem. 67 (1995) 735–743.
[36] G.C. Li, K. Chao, C.S. Ye, H. Peng, One-step synthesis of Ag nanoparticles supported on $AgVO_3$ nanobelts, Mater. Lett. 62 (2008) 735–738.
[37] C.L. Lu, L. Han, W.P. Ding, G. Yang, X.F. Guo, W.H. Hou, In-situ controllable synthesis of Ag nanoparticles: irradiation induced surface segregation of $Ag_2V_4O_{11}$ nanobelt, J. Nanosci. Nanotechnol. 9 (2009) 6554–6559.
[38] S.W. Keller, H.N. Kim, T.E. Mallouk, Layer-by-layer assembly of intercalation compounds and heterostructures on surfaces: Toward molecular "beaker" epitaxy, J. Am. Chem. Soc. 116 (1994) 8817–8818.
[39] P.N. Bartlett, P.R. Birkin, J.H. Wang, F. Palmisano, G. De Benedetto, An enzyme wwitch employing direct electrochemical communication between horseradish peroxidase and a poly (aniline) film, Anal. Chem. 70 (1998) 3685–3694.
[40] E.C. Hurdis, H. Romeyn, Accuracy of determination of hydrogen peroxide by cerate oxidimetry, Anal. Chem. 26 (1954) 320–325.
[41] C. Matsubara, N. Kawamoto, K. Takamura, Oxo[5, 10, 15, 20-tetra(4-pyridyl)porphyrinato]titanium(IV): an ultra-high sensitivity spectrophotometric reagent for hydrogen peroxide, Analyst 117 (1992) 1781–1784.
[42] S.F. Wang, T. Chen, Z.L. Zhang, X.C. Shen, Z.X. Lu, D.W. Pang, Direct electrochemistry and electrocatalysis of heme proteins entrapped in agarose hydrogel films in room-temperature ionic liquids, Langmuir 21 (2005) 9260–9266.
[43] W. Ma, D. Tian, Direct electron transfer and electrocatalysis of hemoglobin in ZnO coated multiwalled carbon nanotubes and nafion composite matrix, Bioelectrochemistry 78 (2010) 106–112.
[44] E. Laviron, General expression of the linear potential sweep voltammogram in the case of diffusionless electrochemical systems, J. Electroanal. Chem. 101 (1979) 19–28.
[45] Y.Z. Xian, Y. Xian, L.H. Zhou, F.H. Wu, Y. Ling, L.T. Jin, Encapsulation hemoglobin in ordered mesoporous silicas: influence factors for immobilization and bioelectrochemistry, Electrochem. Commun. 9 (2007) 142–148.
[46] Y.G. Liu, C.L. Lu, W.H. Hou, J.J. Zhu, Direct electron transfer of hemoglobin in layered α-zirconium phosphate with a high thermal stability, Anal. Biochem. 375 (2008) 27–34.
[47] J.J. Zhang, Y.G. Liu, L.P. Jiang, J.J. Zhu, Synthesis, characterizations of silica-coated gold nanorods and its applications in electroanalysis of hemoglobin, Electrochem. Commun. 10 (2008) 355–358.
[48] Y. Xian, Y. Xian, L. Zhou, F. Wu, Y. Ling, L. Jin, Encapsulation hemoglobin in ordered mesoporous silicas: influence factors for immobilization and bioelectrochemistry, Electrochem. Commun. 9 (2007) 142–148.
[49] Y.D. Zhao, Y.H. Bi, W.D. Zhang, Q.M. Luo, The interface behavior of hemoglobin at carbon nanotube and the detection for H_2O_2, Talanta 65 (2005) 489–494.

Biographies

Chunliang Lu earned PhD degree at Key Laboratory of Mesoscopic Chemistry of MOE, School of Chemistry and Chemical Engineering, Nanjing University in 2009. He is an assistant researcher at Testing Center of Yangzhou University, Yangzhou University. His research focuses on preparation and application of nanomaterials.

Qingming Shen earned PhD degree at Key Laboratory of Mesoscopic Chemistry of MOE, School of Chemistry and Chemical Engineering, Nanjing University in 2008. He is a postdoctoral researcher at Key Laboratory of Analytical Chemistry for Life Science of MOE, School of Chemistry and Chemical Engineering, Nanjing University. His research focuses on ultrasonic electrochemisty and biosensor.

Xiaomei Zhao, PhD student at Key Laboratory of Analytical Chemistry for Life Science of MOE, School of Chemistry and Chemical Engineering, Nanjing University.

Junjie Zhu, professor of analytical chemistry, Vice-Dean of School of Chemistry and Chemical Engineering, Nanjing University. His research focuses on preparation and characterization of nanomaterials, bioelectrochemistry and nanoelectrochemistry.

Xuefeng Guo, associate professor of physical chemistry, School of Chemistry and Chemical Engineering, Nanjing University. His research focuses on novel non-carbon nanotubes, nanocomposites, mesoporous and microporous zeolites, assembly of nanostructrures, and heterogeneous catalysis.

Wenhua Hou, professor of physical chemistry, School of Chemistry and Chemical Engineering, Nanjing University. His research focuses on novel layered materials, nanocomposites, and catalysis.